ELSEVIER

Ceramics International 30 (2004) 539–543

CERAMICS INTERNATIONAL

www.elsevier.com/locate/ceramint

Pulse electric current sintering and microstructure of industrial mullite in the presence of sintering aids

D. Doni Jayaseelan [a,*], D. Amutha Rani [a], D. Benny Anburaj [b], T. Ohji [a]

[a] *Synergy Materials Research Center, AIST, Nagoya 463-8687, Japan*
[b] *Department of Physics, TBML College, Porayar 609307, India*

Received 2 July 2003; received in revised form 28 July 2003; accepted 2 September 2003

Abstract

A commercially available mullite powder with stoichiometric composition was densified by the pulse electric current sintering (PECS) technique at 1500 °C with a holding time of 2 min to produce a fully dense microstructure. Transition metal oxides such as 0.5 wt.% of SrO and 0.2 wt.% MgO were added as sintering aids for mullite. The sintering aids greatly assisted for the modification of mullite grains in the sintered specimens. MgO added mullite exhibited equiaxed morphology, whereas SrO addition led to an equiaxed and anisotropic morphology of mullite grains.

Keywords: A. Sintering; C. Fracture; D. Mullite; Anisotropy; Pulse electric current sintering

1. Introduction

Mullite of stoichiometric ratio (3:2) is one of the most common components of traditional ceramic materials. It is also considered as a candidate material for high temperature applications because of its dependable chemical, thermal, and mechanical properties over a wide range of temperature. Though, mullite has been widely used, the severe impediments to the application of mullite in several advanced structural applications are its poor tendency for densification and low strength, and fracture toughness.

Recently much interest has been focused on the sintering aids of mullite [1–7]. A number of dopants such as MgO, B_2O_3, Fe_2O_3, CeO_2, TiO_2, etc. have been reported to promote the anisotropic grain growth in mullite [4–7]. The dopants primarily aid for the reduction in the viscosity of glassy (or liquid) phase [7] or for the reduction in the mullite formation temperature in gel-derived powders [8], thereby leading to a higher mobility of the diffusing species. From above studies, it is clear that a close compositional and microstructural control is necessary to maximize the densification. This composition-controlled microstructure of mullite ceramics directly controls the mechanical properties of materials. In most conventionally sintered high pure mullite, in which very little or no glassy phase is detected, bend strengths between 250 and 400 MPa at room temperature are reported and these values are maintained up to temperatures ranging from 1200 to 1400 °C. While there is a trade off relation between flexural strength and fracture toughness of monolithic mullite, it is observed in present study that there is a better balance of flexural strength and fracture toughness by the addition of suitable sintering aids. In this work, mullite was doped individually with MgO and SrO, in proper weight ratio. The samples were densified by the pulse electric current sintering (PECS) technique and their room temperature mechanical properties were studied. The fractographic features of mullite were discussed.

2. Experimental procedure

2.1. Materials processing

A commercially available coarse-grained mullite (Kyoritsu Yowgow Co., KM: 102, d_{50}: 1.3 μm) was used as the starting material. Table 1 shows the characteristics of mullite powder used in present study; 0.2 wt.% of MgO and 0.5 wt.% of SrO were used as the sintering aids for mullite and each of the sintering aids was added to a batch of mullite before wet milling. The powders were wet ball

* Corresponding author. Fax: +81-52-739-0136.
E-mail address: daniel-doni@aist.go.jp (D. Doni Jayaseelan).

0272-8842/$30.00
doi:10.1016/j.ceramint.2003.09.005

Table 1
Characteristics of mullite powder

Characteristics	Value	Testing method
Specific surface area (m^2/g)	8.1	BET method
Average particle size, d_{50} (m)	1.3	Laser diffraction method
Crystalline phases (wt.%)		XRD
Mullite	98.9	
Crystobalite	1.3	
Chemical composition (wt.%)		ICP
Al_2O_3	71.4	
SiO_2	28.1	
ZrO_2	0.183	
$Fe_2O_3 + TiO_2 + CaO + Na_2O + K_2O$	~0.065	
Ignition loss (wt.%)	0.44	At 1050 °C/2 h

mixed in an appropriate ratio in polyethylene jar for nearly 24 h in ethanol using alumina balls as grinding media. The milled slurry was dried in a rotary evaporator at 70 °C for 1 h, dried at 110 °C for nearly 24 h, and then screened to pass through #250 mesh sieve.

2.2. Pulse electric current sintering

Sintering experiments were carried out by the PECS technique (Model SPS-1050, Sumitomo Coal Mining Co., Ltd., Kanagawa, Japan). The PECS process has an unique advantage of self-heating system; heat transfer and mass transfer take place simultaneously due to discharges suppose to take place in voids between the particles, which are tremendous driving forces for the preferential neck growth of grains. The sieved powder was packed in graphite die with graphite punches on both sides and rapidly heated to desired temperature (1500 °C) by pulsed electric current under an applied load of 15 MPa in vacuum. The temperature was increased at a rate of 100 °C/min up to the sintering temperature and after holding for 2 min at the sintering temperature, the dc power was shut off to let the system rapidly cool at a rate of >300 °C/min. During sintering, the linear change in shrinkage along the press direction was determined to compute the densification behavior. The temperature was measured with an optical pyrometer focusing on the surface of graphite die but not directly on the specimen, and there probably existed a difference between the temperature of the die and the specimen considering a very fast heating rate and short holding time. The density of the sintered samples was determined by Archimedes method using water as medium.

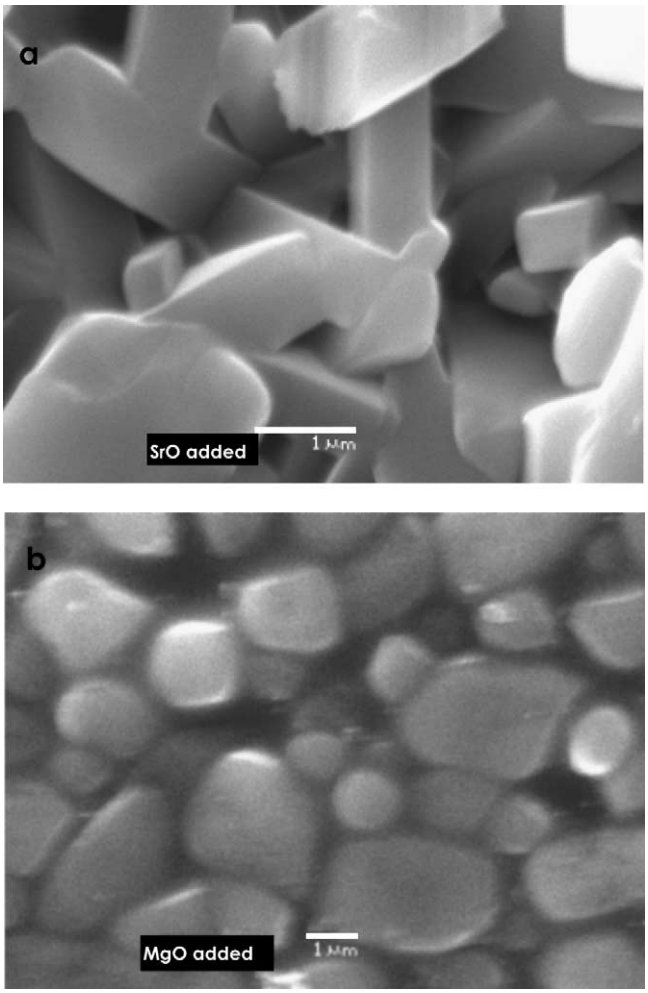

Fig. 1. Microstructures of sintered mullite; the polished surfaces were thermally etched at 1450 °C for 30 min: (a) SrO added mullite and (b) MgO added mullite.

2.3. Mechanical properties

Young's modulus was measured by the pulse echo method. Vicker's hardness was measured by applying a

Table 2
Mechanical properties of mullite compacts

Property	Ref. [11]	Ref. [12]	SrO doped[a]	MgO doped[a]
Sintering temperature (°C)	1580	1550	1500	1500
Sintering condition	PLS	HP	PECS	PECS
% of TD			99	98.3
Flexural strength (MPa)	265 ± 2	320 ± 15	450 ± 50	441 ± 34
Fracture toughness ($MPa\,m^{1/2}$)	2.97 ± 0.37	1.9 ± 0.2	2.9 ± 0.11	2.0 ± 0.75
Vicker's hardness (GPa)		13	13	12.3
Young's modulus (GPa)			223 ± 3	222

PLS–pressureless sintering; HP–hot pressing; PECS–pulse electric current sintering.
[a] Present study.

load of 10 kgf for 15 s on the polished surface of the specimens. The flexural strength was evaluated by three-point bend test for specimens of size 3 mm × 4 mm × 23 mm with a span length of 16 mm and a crosshead speed of 0.1 mm/min. The effective volume has been applied to explain the strength characteristics depending on specimen geometry, by using the well-known Weibull size-scaling relationship [8]. The fracture toughness was estimated by single edge V-notched beam (SEVNB) technique [9] for specimens having dimension of 3 mm × 4 mm × 23 mm, with a span length of 16 mm. For SEVNB specimens, a V-shaped notch introduced by a specially designed diamond wheel had a very sharp root radius of around 10 μm with a notch angle less than 30°. Three-point bend test was carried out for V-notched specimens under mode-I loading. The microstructure of the tensile surface and the fractured surface was observed using scanning electron microscope (SEM, Model—LEICA STEREOSCAN S440).

3. Results and discussion

Pulse electric current sintering of industrial mullite at 1500 °C for 2 min and under an applied load of 15 MPa reproducibly yielded cylindrical disks (30 mm diameter, 10 mm height) with density greater than 98% of the

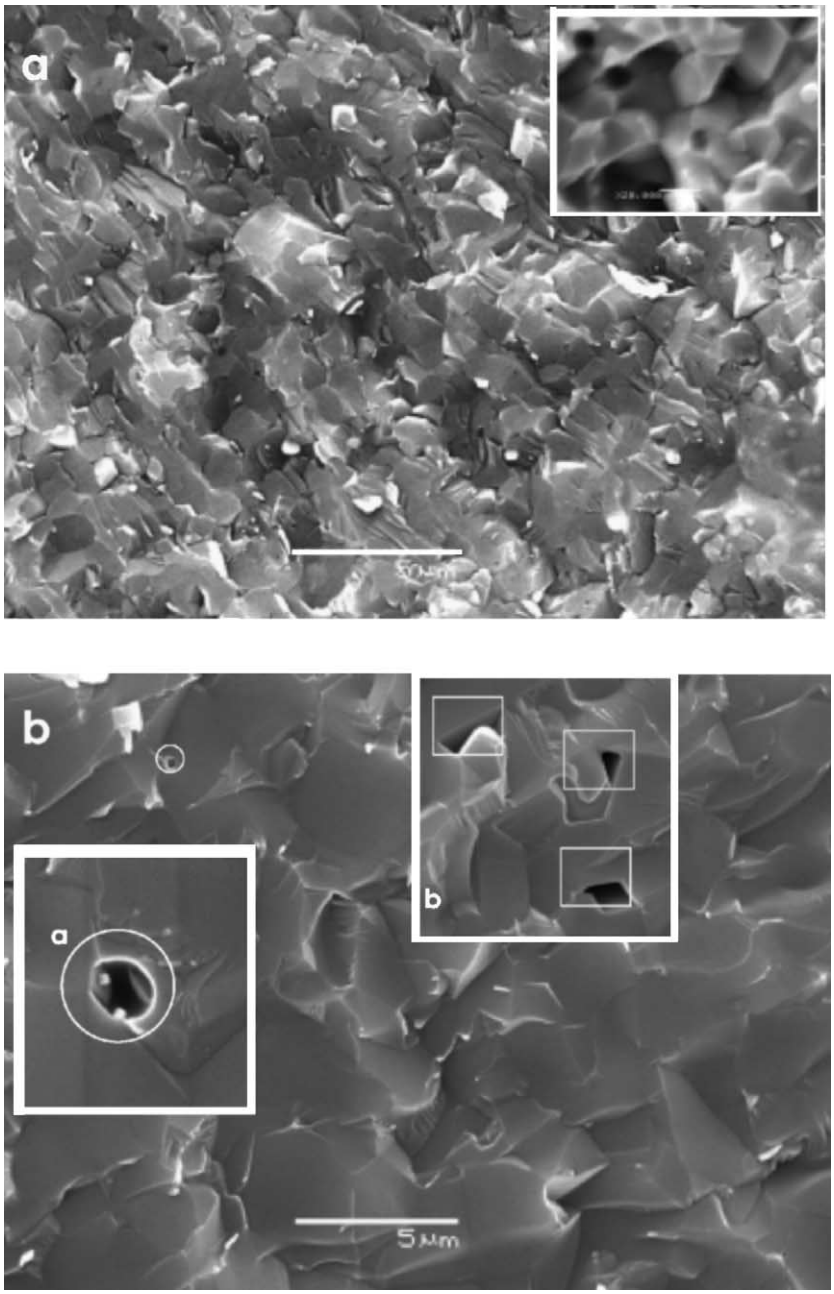

Fig. 2. Fracture surface of mullite: (a) SrO added mullite (insert shows typical intergranular fracture) and (b) MgO added mullite.

theoretical density [10]. Table 2 shows the mechanical properties of the sintered industrial mullite specimens. Both SrO and MgO added mullite in our present study showed better mechanical properties when compared with previous studies [11,12]. Although, previous study [11] reported higher fracture toughness (because of the elongated morphology of mullite grains) than in the present study, the strength was as low as 265 MPa. In present study, there is a better balance of flexural strength, 450 MPa (393–503 MPa) and fracture toughness, 2.9 MPa $m^{1/2}$, for mullite compacts. The increase in flexural strength must be related to finer microstructure of mullite compacts sintered by the PECS technique. As a factor to influence the fracture toughness, the difference in grain size should be considered. The grains of SrO and MgO added sintered mullite compacts are similar in size; the grain size is not directly associated with the change in fracture toughness in the present case.

Fig. 1a and b show the microstructures of thermally etched SrO and MgO added mullite compacts sintered at 1500 °C, respectively. The sintered mullite compacts had relatively finer microstructure. Mullite compact sintered with SrO showed a duplex microstructure consisting of very fine equiaxed and elongated grains. The microstructure of MgO added mullite shows equiaxed, and the grains are observed to be smoother. There was no appreciable grain growth, when considering the particle size (1.3 μm) of the starting material.

Fig. 2a and b show the fracture surfaces of SrO doped and MgO doped mullite, respectively. Growth of rod-like particles in the SrO added mullite changed the fracture mode from mainly transgranular to the mixed type of intergranular and transgranular in monophasic mullite ceramics. Though, a lower magnification micrograph showed predominantly transgranular mode of fracture, fracture also occurred along the grain boundaries in some places (see the insert). On experiencing a grain boundary fracture, the area of fracture increased and it could absorb much more energy. Therefore, the growth of rod-like mullite should increase the fracture energy of mullite ceramics. This is for the reason that SrO added mullite compacts exhibited higher fracture toughness when comparing MgO added mullite. In this approach, an enhancement of the fracture toughness of the monolithic ceramic is achieved by the development of an interlocking microstructure of elongated grains [12]. Hence, it is fair to relate the fracture toughness to the corresponding changes in the microstructure and the fracture mode due to the addition of sintering aids.

MgO added mullite showed completely typical transgranular mode of fracture (Fig. 2b). Some holes or pores were present in the fractured surface. It is also noted that these pores varied in size from very small to large. The spherical pores (insert 'a') might be originated during sintering of mullite compact. Conversely, sharp-edged pores (insert 'b') might be due to diffusion at high temperatures, which can lead to clustering and collapse of vacancies at grain boundaries. In region near the sharp-edged pores and

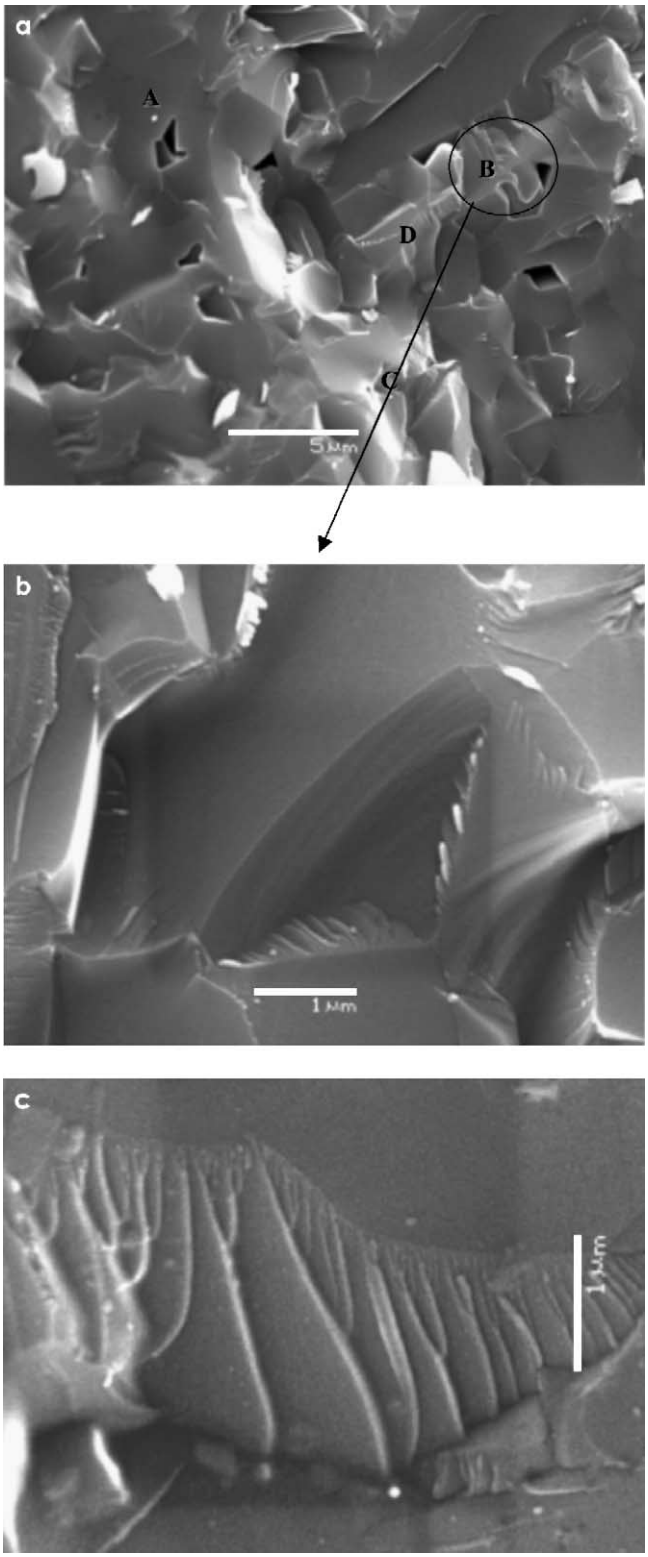

Fig. 3. Fracture surface of MgO added mullite: (a) fracture surface of mullite showing spherical and sharp-edged pores and surface marking; (b) higher magnification showing cleavage steps; and (c) micrograph of the formation of a 'river pattern' of steps after passage of grain boundary (MgO added mullite).

in many other areas, surface markings and cleavages were also observed. An example of this is shown in Fig. 3a. Area A is a sharp-edged pore. The grain B has extensively cleaved, and the regions C and D in other grains show some cleavage. A magnified view of surface markings is shown in Fig. 3b and these surface markings are believed to be the cleavage planes. The presence of sharp-edged pores at grain boundaries and grain boundary junctions is found to favor the cleavage, with the pores acting as stress concentrators [13]. Fig. 3c is a typical 'river pattern', which occurred in the samples. River pattern often forms at the passage of a grain boundary [16]. As neighboring grains may have slightly different orientations, the cleavage crack changes direction at a grain boundary to continue propagation on the preferred cleavage plane. Within a grain, a crack may grow simultaneously on two parallel crystallographic planes. The two parallel cracks join along the line where they overlap, either by secondary cleavage or by shear to form a step [14,15]. A number of cleavage steps may join and form a multiple step; cleavage steps of opposite sign may join and disappear. Merging of cleavage steps results in a 'river pattern' so called because of its resemblance to a river and its tributaries. Hence, high fracture toughness values in the MgO added sample ($\sim$2.75 MPa $m^{1/2}$) must be related to the additional toughening from the formation of cleavage steps. Step formation restraints the propagation of brittle cracks by absorbing extra energy in the vicinity of the connecting stress-riser between adjacent crack planes.

4. Summary

The PECS of industrial mullite at 1500 °C for 2 min reproducibly yielded mullite compacts of near theoretical density. The dopants influenced the morphology of mullite grains and hence the fracture mode. The PECS sintered mullite compacts exhibited a better balance of strength and fracture toughness, i.e. the strength and fracture toughness of mullite were increased to 450 ± 50 MPa and 2.9 ± 0.1 MPa $m^{1/2}$, respectively. The fracture toughness exhibited a slight dependency on the mode of fracture. The fracture surface of MgO added mullite was highly crystallographic in nature and the grains showing extensive fine cleavage were observed.

Acknowledgements

The authors D.D.J., D.A.R. and T.O. thank the support of METI as part of the Synergy Ceramics Project and are members of the Joint Research Consortium of Synergy Ceramics Project.

References

[1] M.G.M.U. Ismail, H. Tsunatori, Z. Nakai, Preparation of MgO-doped mullite by sol–gel method, powder characteristics and sintering, J. Mater. Sci. 25 (1990) 2619–2625.
[2] L. Montanaro, C. Perrot, C. Esnouf, G. Thollet, G. Fantozzi, A. Negro, Sintering of industrial mullites in the presence of magnesia as a sintering aid, J. Am. Ceram. Soc. 83 (1) (2000) 189–196.
[3] D. Amutha Rani, D. Doni Jayaseelan, F.D. Gnanam, Densification behavior and microstructure of gel-derived phase pure mullite in the presence of sinter additives, J. Eur. Ceram. Soc. 21 (2001) 2253–2257.
[4] H. Schneider, Transition metal distribution in mullite, Ceram. Trans. 6 (1990) 135–158.
[5] S.-H. Hong, W. Cermignani, G.L. Messing, Anisotropic grain growth in seeded and B_2O_3-doped diphasic mullite gels, J. Eur. Ceram. Soc. 16 (1996) 133–141.
[6] S.-H. Hong, G.L. Messing, Anisotropic grain growth in diphasic-gel-derived titania doped mullite, J. Am. Ceram. Soc. 81 (5) (1998) 1269–1277.
[7] P. Mechnich, M. Schmucker, H. Schneider, Reaction sequence and microstructural development of CeO_2-doped reaction-bonded mullite, J. Am. Ceram. Soc. 82 (9) (1999) 2517–2522.
[8] D.G.S. Davies, Proc. Br. Ceram. Soc. 22 (1973) 429.
[9] H. Awaji, Y. Sakaida, V-notch technique for single edge notched beam and chevron notch methods, J. Am. Ceram. Soc. 73 (11) (1990) 3522–3523.
[10] D. Doni Jayaseelan, D. Amutha Rani, T. Nishikawa, H. Awaji, T. Ohji, Sintering and microstructure of mullite/Mo composites, J. Eur. Ceram. Soc. 22 (7) (2002) 1113–1117.
[11] J. Meng, S. Cai, Z. Yand, Q. Yuan, Y. Chen, Microstructure and mechanical properties of mullite ceramics containing rod like particles, J. Eur. Ceram. Soc. 8 (1998) 1107–1114.
[12] J.F. Bartolome, M. Diaz, J. Requena, J.S. Moya, A.P. Tomsia, Mullite–molybdenum composites, Acta Mater. 47 (1999) 3891.
[13] R. Torrecillas, J.M. Calderon, J.S. Moya, M.J. Reece, C.K.L. Davies, C. Olagnon, G. Fantozzi, Suitability of mullite for high temperature applications, J. Eur. Ceram. Soc. 19 (1999) 2519–2527.
[14] J.R. Low, A review of the microstructural aspects of cleavage fracture, in: Fracture (Swampscott Conference), 1959, pp. 68–90.
[15] J. Friedel, Propagating cracks and work hardening, in: Fracture (Swampscott Conference), 1959, pp. 498–523.
[16] C.D. Beachem, Microscopic fracture processes, in: Fracture I, Academic Press, Liebowitz, 1968, pp. 243–349.